J. King Saud Univ., Vol. 13, *Eng. Sci.* (2), pp.205-225 (A.H. 1421/2000)

Capability Diagram of Dual-field Alternators Including Magnetic Saturation

A.A. Al-Ohaly and M.A. Abdel-Halim
Electrical Engineering Department, King Saud University
P.O. Box 800, Riyadh 11421, Saudi Arabia

(Received 20 November, 1999; accepted for publication 26 April, 2000)

Abstract. The dual-field alternators have been developed to improve the stability of the power systems. This paper presents an accurate study of the dynamic stability of such alternators. Assessment of stability is performed based on calculation of the synchronizing and damping torque coefficients. The alternator is represented by a detailed circuit model which incorporates properly the saturation effects. Based on this model, the torque coefficients have been calculated using a least square algorithm which is applied to the time responses of the mechanical variables. Boundaries of the dynamically stable operation regions have been determined under the action of both the automatic voltage regulator; AVR and the automatic angle regulator, AAR. Then, the thermal limits imposed by the heating problem and the mechanical limits imposed by the mechanical system have been incorporated to determine the capability diagram of the dual-field alternator.

List of Symbols

E : induced voltage, p.u
i : current, p.u
H : inertia constant, sec.
K_d, K_s : damping and synchronizing torque coefficients
p : normalized time derivative operator
T_e : electromagnetic torque, p.u
V_a : alternator terminal voltage, p.u
V : bus bar terminal voltage, p.u
ψ : flux linkage, p.u
θ : rotor position, electrical radians
δ : rotor angle, electrical radians
μ : saturation factor
ω_o : base speed, rad/sec
γ : field copper loss ratio

Subscripts

1,2,... : damper circuit numbers
a,f,k : armature, field and damper respectively
b,r : bar and ring respectively
d,q : direct and quadrature-axis respectively
h : harmonic
l : leakage

Superscripts

s : static saturated
u : unsaturated
* : dynamic saturated

Introduction

The dynamic stability margin of dual-field alternators is clearly improved by using an automatic voltage regulator; AVR, on the d-axis field and an automatic angle regulator; AAR, on the q-axis field [1-5]. This paper studies the dynamic stability of a saturated dual-field alternator connected to an infinite bus-bar through a short tie line (Fig.1). The study aims at determining the stable operating regions. These, together with the constraints imposed on the alternator operation regions by the thermal and mechanical endurance limits, are used to determine the machine capability diagram.

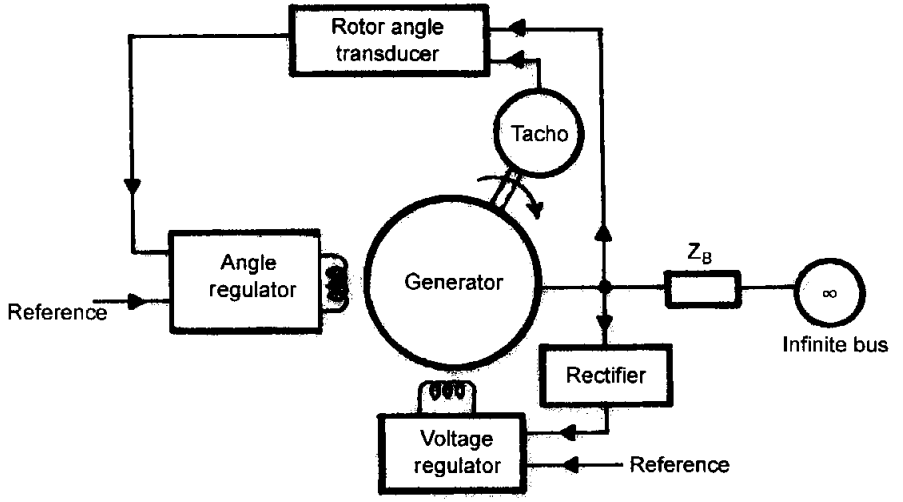

Fig. 1. Schematic diagram of the dual - excited alternator.

Synchronizing and damping torque coefficients have been used to evaluate the dynamic stability of alternators since 1927 [6-8]. Many attempts have been done to improve both the method of calculation of these coefficients [6-8] and the model representing the machine [8-13]. Previous authors [11-13] have adopted the conventional equivalent circuit to model the dual excited alternator. This model represents the damper winding approximately by one lumped coil on each axis. Also, it assumes equal mutual reactances between the armature, field and damper windings in each axis. This is corrected in the present paper by representing the machine in the dqo reference frame by detailed circuit model based on the features of Linville-Rankin equivalent circuits [14,15].

The performance of the dual-field alternator like the other electrical machines is greatly affected by the magnetic saturation. Nevertheless, most of the previous publications [5,16] have neglected the electromagnetic nonlinearity effects, while others [2,11,12] consider the saturation based on the open circuit characteristic. All these authors assume that only the mutual reactances are influenced by saturation, while the leakage reactances are assumed unsaturable. Harley [12] assumes different d- and q- axis saturation levels neglecting the mutual d/q saturation effects because of the saliency effects. On the other hand, Kapoor [2] and Soper [11] assume the same degree of saturation in both axes which is determined corresponding to the resultant flux. Considerable error has been introduced by most of the previous authors as they use the saturated chord reactances to calculate both the rotational and transformer voltage terms of the equation describing the machine performance. Kapoor [2] avoided this error by using chord reactance for rotational voltage and incremental reactance for transformer voltage. In this paper, saturation is treated using a developed method that considers mutual saturation effects between the main and leakage fluxes. Also, two different values of each saturated reactance are used according to the voltage term in which it appears; a static saturated reactance for the rotational voltage and dynamic saturated reactance for the transformer voltage [16].

Principle of Excitation

Previous literatures [7,8] have shown that the AVR of a single-excited alternator gives a positive synchronizing torque component when the alternator supplies high active power together with high capacitive reactive power. At other loading conditions, the AVR gives negative synchronizing torque component. The effect of the AVR on the damping torque is such that it gives a negative damping torque component except when the alternator is supplying low active power together with high capacitive reactive power. The effect of the regulator regarding the synchronizing and damping torque is nearly canceled when the machine delivers or absorbs pure reactive power. In this case, the rotor d-axis nearly coincides with the resultant air gap flux.

Accordingly, the dual-excited machine field excitations are adjusted such that the rotor d-axis coincides with the axis of the resultant air gap flux. The q-axis excitation, in this case, provides the excitation that balances the armature reaction component in the q-axis. This, together with controlling the q-axis excitation through a rotor position signal; δ, will improve the dynamic stability limits of the dual-excited alternator. Figure 2 shows the voltage phasor diagrams of both the single-field and the dual-field alternators.

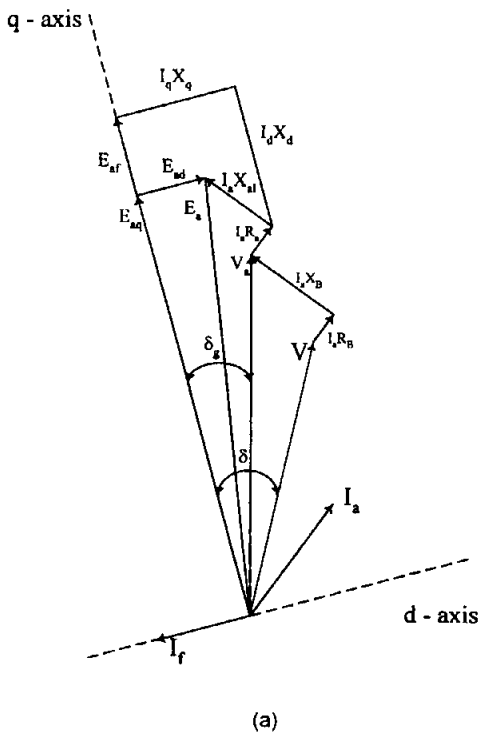

Fig. 2-a. Single-field alternator phasor diagram.

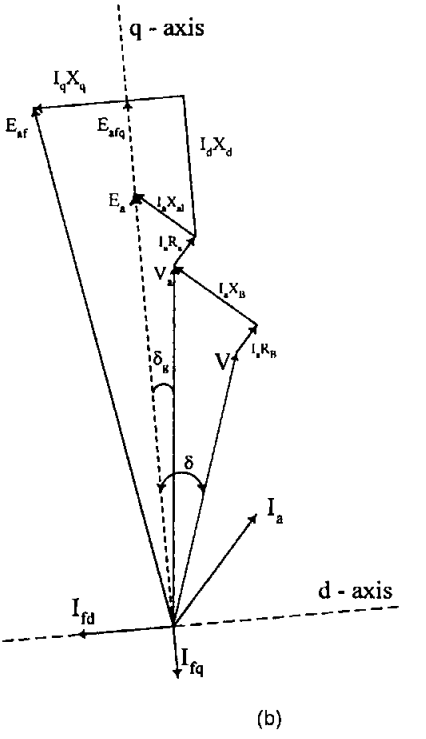

Fig. 2-b. Dual-field alternator phasor diagram.

Modelling of the System

Modelling of the alternator

Linville-Rankin equivalent circuits [14,15] have been adopted to represent the dual-excited alternator. The q-axis circuit has been modified to represent the additional q-axis field coil. Figure 3 shows these equivalent circuits for an arbitrary number of damper bars equal to five bars per pole shoe. The developed circuit has the following advantages:

i) it represents the mutual coupling between the rotor coils properly through the total air gap flux instead of the fundamental flux only.
ii) the damper winding is represented accurately by several nested coils on both axes.
iii) Ideal transformers appear in the equivalent circuit to avoid wrong coupling between the field coils and damper coils through the end ring segments.
iv) the parameters are developed using the MMF-base per-unit system [14] which leads to discrete mutual reactances. This enables individual treatment of each saturable reactance.

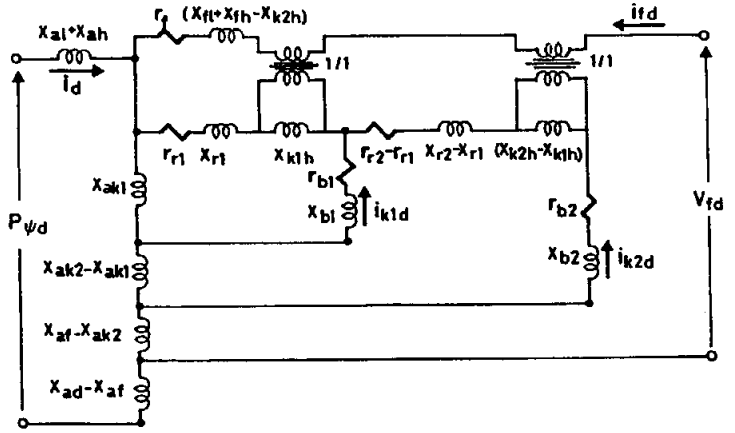

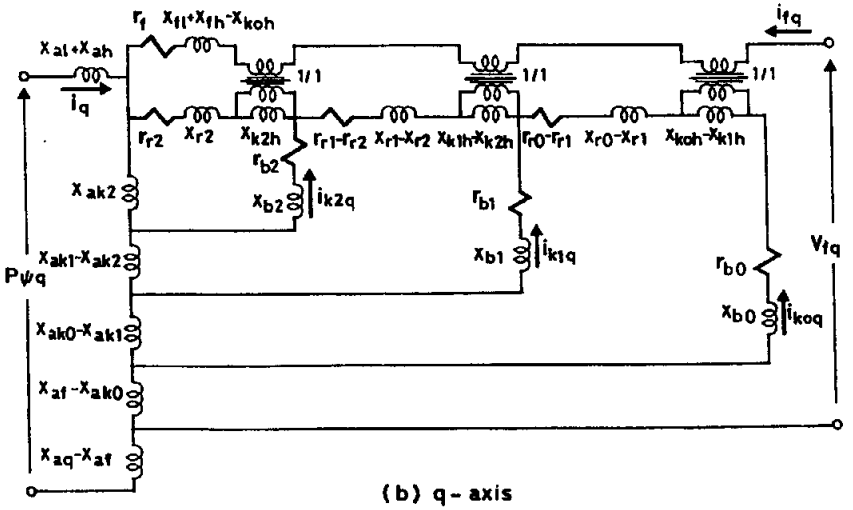

Fig. 3. Equivalent circuit.

The dynamic performance of the system is governed by the following equations:

$$[v] = [R][i] + [x]p[i] + p\theta\,[G][i] \tag{1}$$

$$T_m = T_e + 2\omega_o H\, p^2\delta \tag{2}$$

$$p\theta = 1 + p\delta \tag{3}$$

where;

$$[v] = [v\sin\delta, v_{fd}, 0, 0, \ldots, -v\cos\delta, v_{fq}, 0, 0]^T \tag{4}$$

$$[i] = [i_d, i_{fd}, i_{kld}, i_{k2d}, \ldots, i_q, i_{fq}, i_{klq}, i_{k2q}, \ldots]^T \tag{5}$$

$$T_e = \psi_d i_q - \psi_q i_d \tag{6}$$

The mechanical torque of the prime-mover; T_m, is considered constant during a small oscillation of the alternator around the steady-state point. [R], [x] and [G] are the alternator resistance, transformer-voltage reactance and rotational-voltage reactance matrices respectively. The tie-line resistance and reactance are added to the armature resistance and leakage reactance respectively.

Modelling of the regulators

V_{fd} in the alternator equation is governed by the AVR, while V_{fq} is governed by the AAR. Static types of these regulators are used to control the dual excited alternator. With the aid of the IEEE excitation models [17], the regulators are modelled by the block diagrams shown in Figs. 4 and 5.

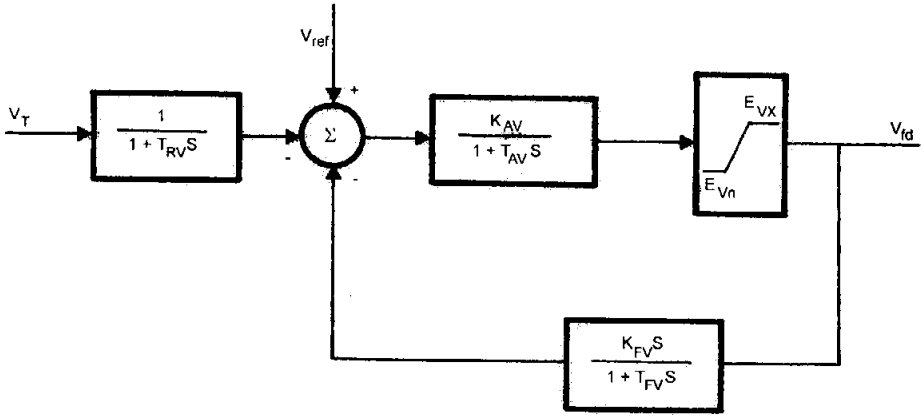

Fig. 4. Block diagram of the AVR.

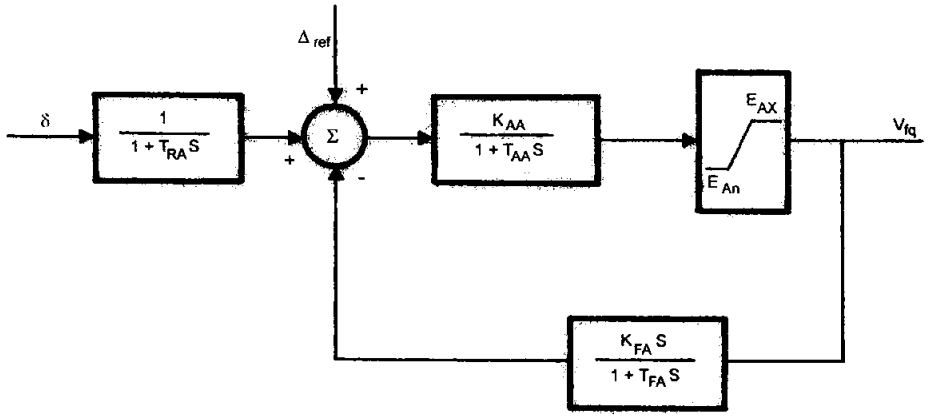

Fig. 5. Block diagram of the AAR.

Saturation representation

As the magnetization characteristics of the alternator iron core are not linear, the reactances of its circuit model are not constant. These will be affected by the saturation of the iron. Accurate representation of saturation in the dual-excited alternator is based on the following points:

i) Saturation affects the direct-axis of the machine only. The q-axis is considered unsaturated as the suggested excitation sharing between the two field windings results in a zero q-axis flux. Also, the machine saliency is a diminishing factor for the mutual saturation effects between the d- and q-axis fluxes [8,16].

ii) Mutual saturation exists between the d-axis main and leakage fluxes [16]. Thus, all the main and leakage reactances are affected by saturation. It is believed that the saturation has slight effect on the leakage reactances of the damper bars. Therefore it will be neglected.

iii) The linkage fluxes are calculated using static-saturated reactances. Each is related to the unsaturated reactance through a relevant saturation factor such that;

$$X^s = \mu x^u \tag{7}$$

These static saturated reactances are used in the rotational voltage term of the machine equation.

iv) Calculation of the transformer voltage term necessitates the derivation of dynamic saturated reactances to avoid the error introduced by previous authors who used

$$p[\psi] = p\{x^S][i]\} = [x^S]p[i] \tag{8}$$

which is corrected by using a dynamic saturated matrix; $[x^*]$, in place of $[x^s]$ such that;

$$p[\psi] = p\{[x^S][i]\} = [x^*]p[i] \tag{9}$$

Taking the previous points into account, the direct axis saturation factors for the main and leakage static saturated reactances are formulated as follows [8];

$$\mu_{ad}(\text{for } x_{aad} \text{ and } x_{ad}) = \frac{R_{gFd}}{R_{gFd} + \sigma_{Sd} R_{SFd} + R_{PF}}$$

$$\mu_{fd}(\text{for } x_{afd} \text{ and } x_{ffd}) = \frac{R_{gFd}}{R_{gFd} + R_{SFd} + \sigma_P R_{PF}}$$

$$\mu_{kd}(\text{for } x_{kknd} \text{ and } x_{aknd}) = \frac{R_{gFd}}{R_{gFd} + R_{SFd} + R_{PF}}$$

$$\mu_{ald}(\text{for } x_{ald}) = 1 - \frac{\sigma_{Sd} R_{gFd}}{R_{gFd} + \sigma_{Sd} R_{SFd} + R_{PF}} \frac{\lambda_{st}}{\lambda_a}$$

$$\mu_{fld}(\text{for } x_{fld}) = 1 - \frac{\sigma_P R_{PF}}{R_{gFd} + R_{SFd} + \sigma_P R_{PF}} \tag{10}$$

R_{gFd} is the direct-axis air gap reluctance to the flow of the fundamental flux. R_{SFd} and R_{PF} are the direct-axis stator and rotor reluctance to the flow of the fundamental flux respectively. These are obtained from the relevant magnetization curves corresponding to the sum of the main and leakage fluxes flowing in the respective part. σ_{Sd} and σ_P are the stator and rotor leakage flux coefficients respectively. λ_{st} is the slot plus the tooth leakage flux permeance, while λ_a is the armature total leakage flux permeance.

The elements of the dynamic matrix $[x^*]$ are calculated in terms of the elements of the static matrix $[x^S]$ as follows [16];

$$x^*_{jw} = x^s_{jw} + \sum_{m=1}^{N} i_m \frac{\partial x^s_{jm}}{\partial i_w} \tag{11}$$

where N is the matrix order, j and w specify the element position.

Assessment of the Dynamic Stability

The synchronizing and damping torque coefficients are used as indices for the dynamic stability. Whenever one of these is negative, the alternator is unstable. The damping and synchronizing torque components can be obtained by resolving the alternator torque variation around a steady-state point into two components related to its speed variation and rotor angle variation as follows [8],

$$\Delta T_e(t) = k_d \Delta \Delta T_e(t) = k_d \Delta\dot{\theta}(t) + k_s \Delta\delta(t)\,(t) + k_s \Delta\delta(t) \tag{12}$$

Having the small oscillation time responses of the torque, speed and rotor angle, a least square error algorithm is applied to determine both K_s and K_d [8]. This algorithm yields the following equation,

$$\Sigma \Delta T_e(t).\Delta\delta(t) = k_S \Sigma \Delta\delta^2(t) + k_d \Sigma \Delta\dot{\theta}(t).\Delta\delta(t) \tag{13}$$

$$\Sigma \Delta T_e(t).\Delta\dot{\theta}(t) = k_S \Sigma \Delta\dot{\theta}(t)\Delta\delta(t) + k_d \Sigma \Delta\dot{\theta}^2(t) \tag{14}$$

Solving these equations, K_s and K_d are obtained for any steady state operating point.

Electrical Loading and Heating Problem

The armature and field copper losses beside the core losses are the major source of heat inside the alternator. The armature copper loss is controlled by keeping the armature current not more than the rated value. The field copper losses of the dual-field machine depend on both the d- and q-axis field currents. If saturation and saliency are neglected, the d-axis field current of the dual-field alternator will be the component of the field current of the single-field alternator in the new d-axis direction of the dual machine. So, I_{fd} of the dual-field alternator is less than I_f of the single-field alternator. When saturation is considered, the d-axis for both single-field and dual-field alternators are greatly affected but to different degrees. The d-axis saturation level in the dual alternator will correspond to the resultant air gap flux which produces E_a, while in the single alternator the level is less, and will correspond to the flux which produces E_{aq} (Fig.2). Although I_{fd} of the dual alternator is required to produce E_{afq}, while I_f of the single alternator is required to produce the higher voltage E_{af}, the higher saturation level of the dual causes I_{fd} to approach the value of I_f. On the other hand, the q-axis of the dual machine is not affected by saturation. At low lagging power factor, the q-axis field current is approximately equal to the component of the field current of the unsaturated single field alternator in the new q-axis direction of the dual machine. In general, I_{fq}, should give the ampere-turns that balance the effect of I_q.

If the resistances of the two fields of the dual machine are the same, and equal to that of the field of the single-field machine, the field copper loss ratio; γ, of the two machines is estimated as follows:

$$\gamma = \left(I_{fd}^2 + I_{fq}^2\right) / I_f^2$$

No heating problem exists if γ is less or very near to unity. If $\gamma > 1$, more heat is produced in the dual machine compared with a single machine of the same rating.

Results and Discussions

A 494 KVA dual-excited alternator has been chosen for the present study. The alternator and its regulator parameters are given in Appendix 9. A computer program have been developed to simulate the alternator. Using the program, the synchronizing and damping torque coefficients of the alternator have been computed for wide range of operating conditions. The alternator is disturbed from its steady-state through a small step change in its prime-mover torque. The coefficients have been determined including the action of the AVR while the AAR is either:

i) not activated,
ii) activated with negative feed-back rotor position signal, or
iii) activated with positive feed-back rotor position signal.

Samples of the results are shown in Figs. 6 and 7 for two extreme power limits. These results show that the action of the AAR with positive feed-back is acceptable over all the operating range, while the negative feed-back leads to unstable operation at leading power factor operating conditions. The torque coefficients including saturation effects are shown in Figs. 8 and 9. Saturation results in slight increase in the values of the synchronizing torque coefficient, and on the other side slight decrease in the values of the damping torque coefficient. Effect of the variation of the value of the ARR forward gain; K_{AA}, on the alternator stability has been examined. The results are shown, as an example, for loading conditions of zero active power and different reactive powers in Figs. 10 and 11. It is clear that for a positive feed-back action of the AAR, increasing the value of K_{AA} improves the synchronizing torque coefficients only at no-load conditions accompanied by high leading reactive power. On the other side, the damping torque coefficients decrease for all loading conditions with the increase of K_{AA}. For negative feed-back action of the AAR, both K_s and K_d increase slightly with K_{AA} at lagging power factor condition, and decrease noticeably with K_{AA} at leading power factor conditions. The effect of the second field winding with positive feedback on the alternator stability is examined by comparing the values of both K_s and K_d when this winding is excited with those obtained when only the d-axis winding is excited. The results are shown in Figs. 12 and 13 at different loading conditions. It is clear that the q-axis winding improves noticeably the synchronizing torque coefficient, and also improves the damping torque coefficient except at light load conditions.

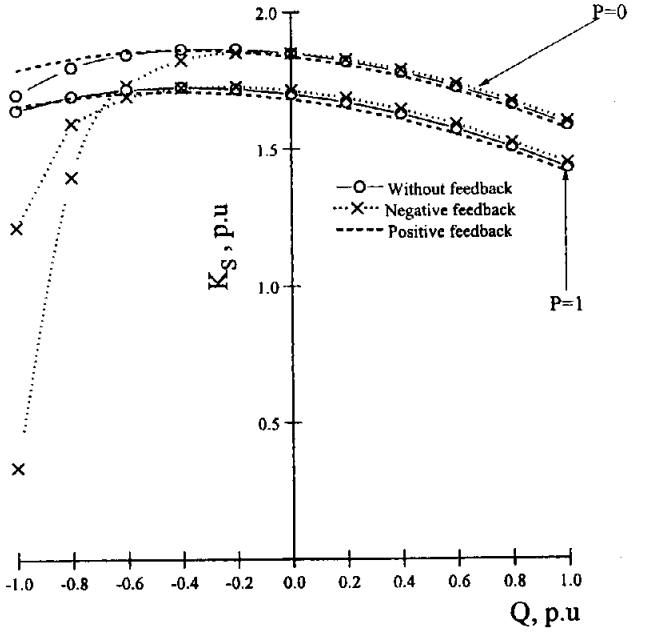

Fig. 6. Synchronizing torque coefficients neglecting the saturation.

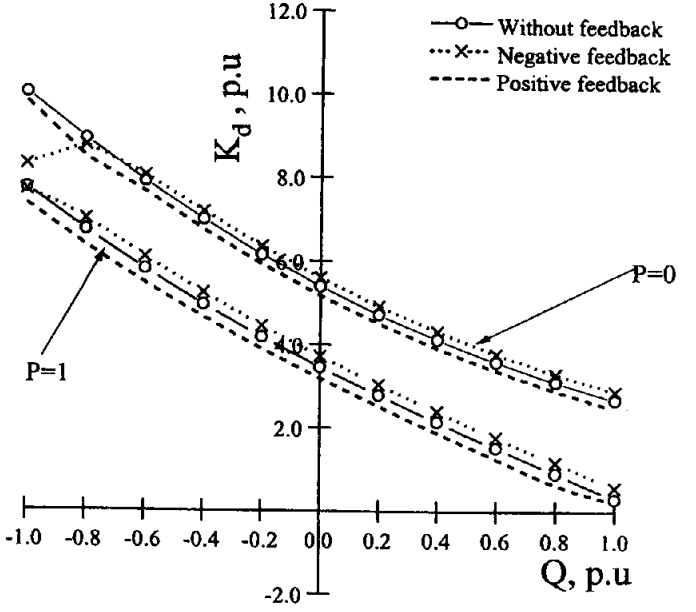

Fig. 7. Damping torque coefficients neglecting the saturation.

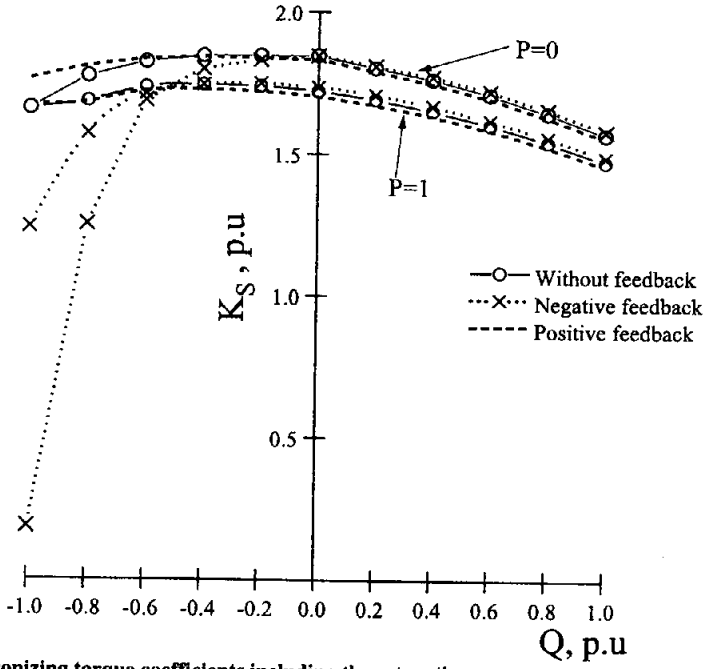

Fig. 8. Synchronizing torque coefficients including the saturation.

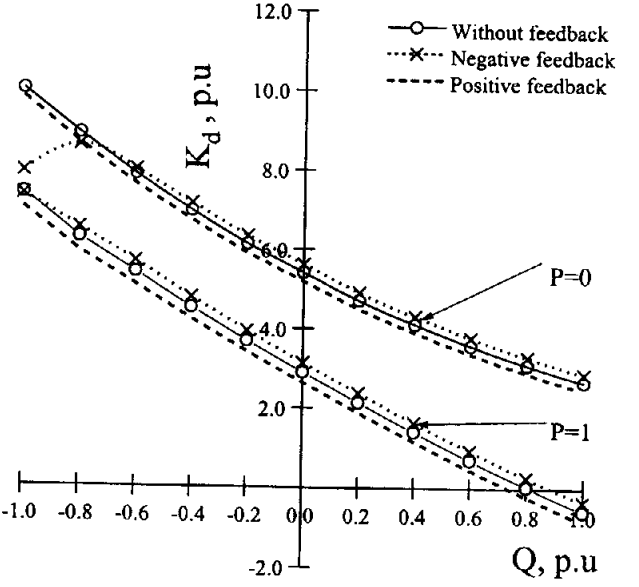

Fig. 9. Damping torque coefficients including the saturation.

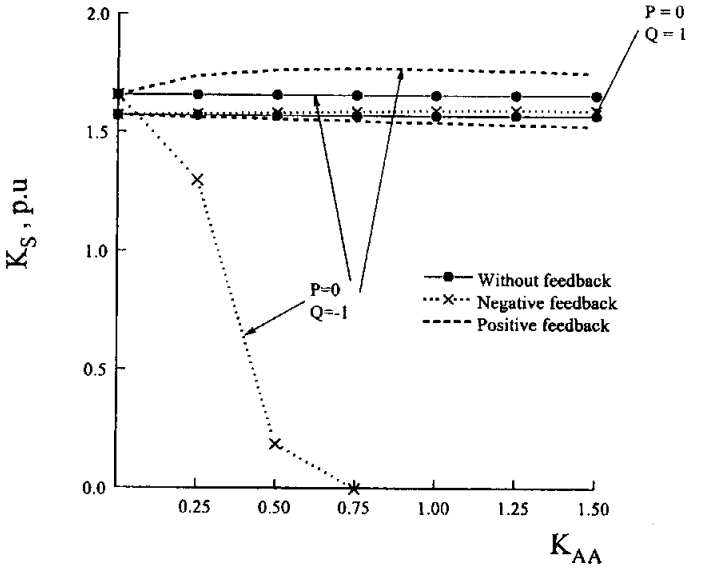

Fig. 10. Variation of synchronizing torque coefficient with K_{AA}.

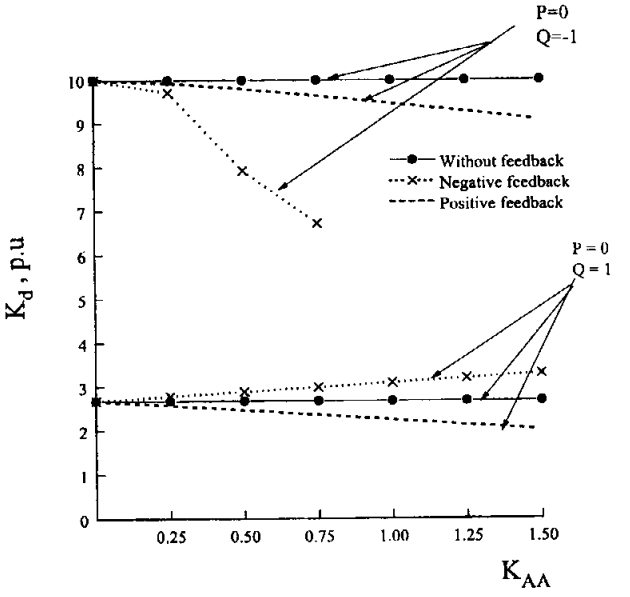

Fig. 11. Variation of damping torque coefficient with K_{AA}.

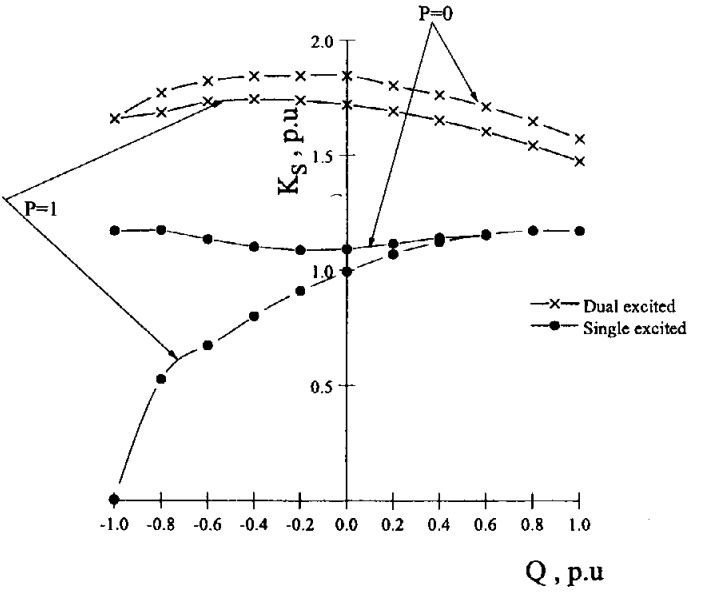

Fig. 12. Synchronizing torque coefficient of a dual-field alternator compared with a single-excited alternator.

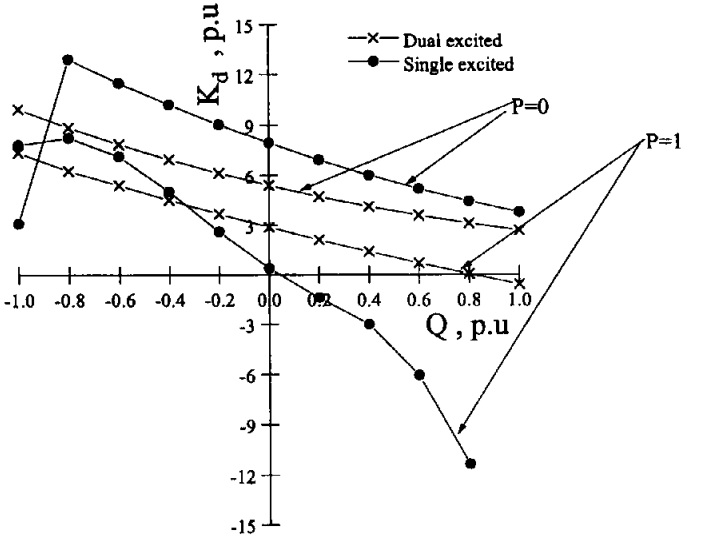

Fig. 13. Damping torque coefficient of a dual-field alternator compared with a single-excited alternator.

To investigate the heating problem associated with field currents of the dual-field alternator, the field currents have been computed for a wide range of operating conditions considering and neglecting the saturation. Figures 14 and 15 show that neglection of the magnetic saturation leads to great error in the predicted values of the d-axis field current for both single and dual-field alternators. When saturation is considered, the field currents increase and the d-axis field current of the dual-field alternator approaches that of the single-field alternator. The variation of the q-axis field current of the dual machine with loading condition is shown in Fig. 16. To compare the field copper losses, the ratio γ has been computed considering saturation, and depicted in Fig.17. In general, the dual losses are higher.

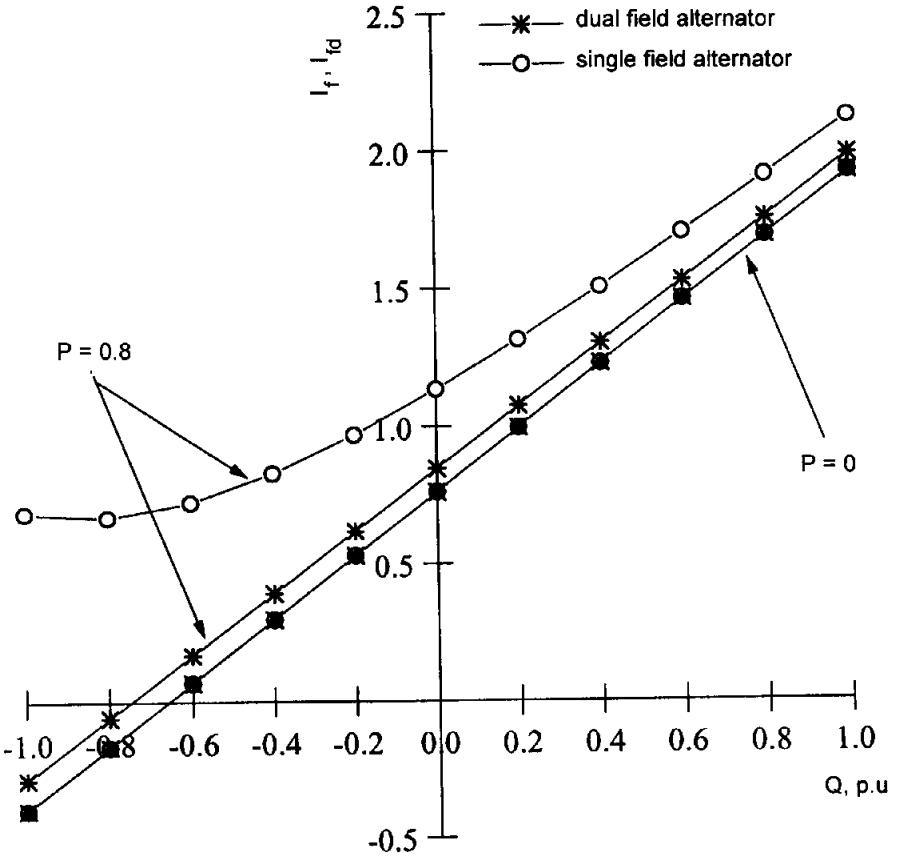

Fig. 14. D-axis field currents neglecting saturation.

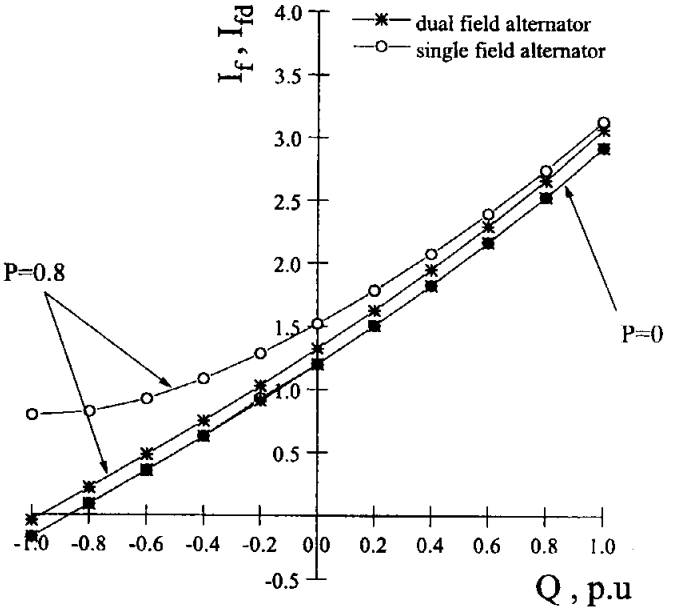

Fig. 15. D-axis field currents considering saturation.

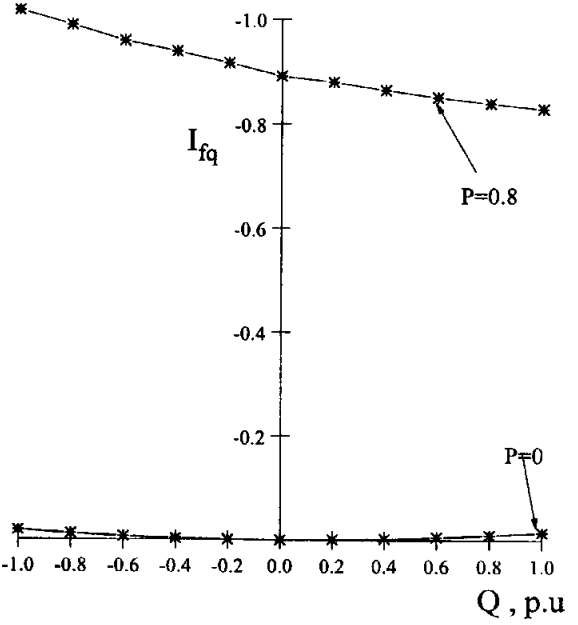

Fig. 16. Q-axis field currents for the dual-field alternator.

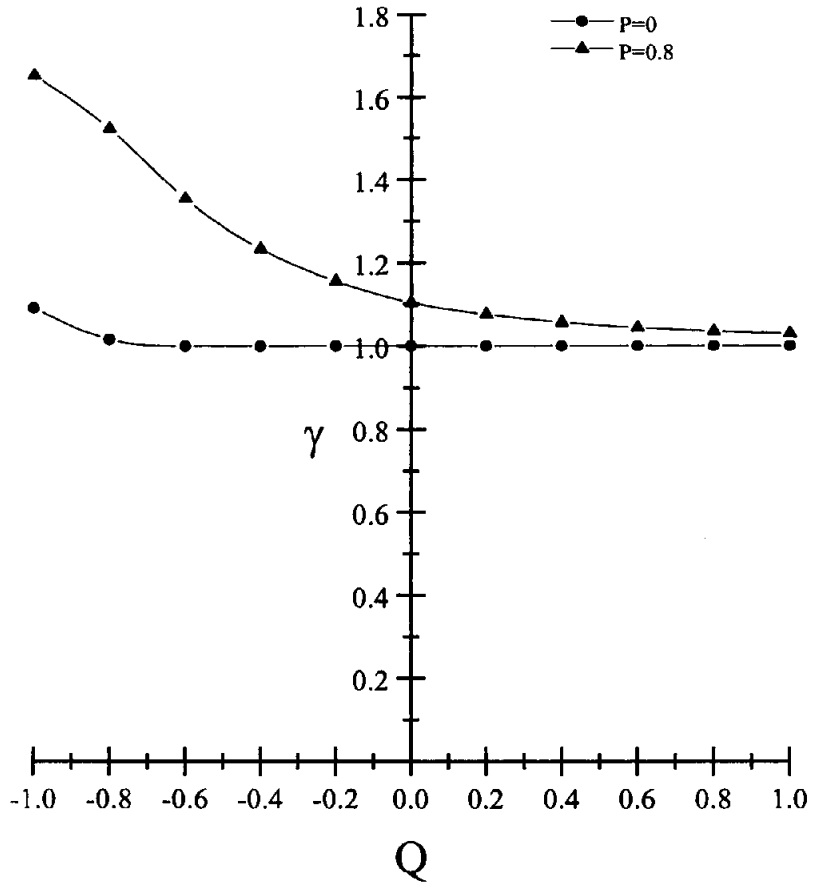

Fig. 17. Variation of the ratio γ with the reactive power.

A capability diagram for the dual field alternator has been developed as shown in Fig.18(a). This diagram is based on the following limits:

- The armature current not to exceed 1.0 p.u.
- The direct-axis field current not to exceed 2.6 p.u (the rated value of this coil if the machine is single excited).
- The quadrature-axis field current not to exceed 1.14 p.u (suitable chosen value).
- The prime-mover power limit is 0.9 p.u.

It worths to mention that the stability limits are outside the operating region, which confirms the advantage of the dual alternator if compared with the capability diagram of the single-excited alternator (Fig. 18(b)).

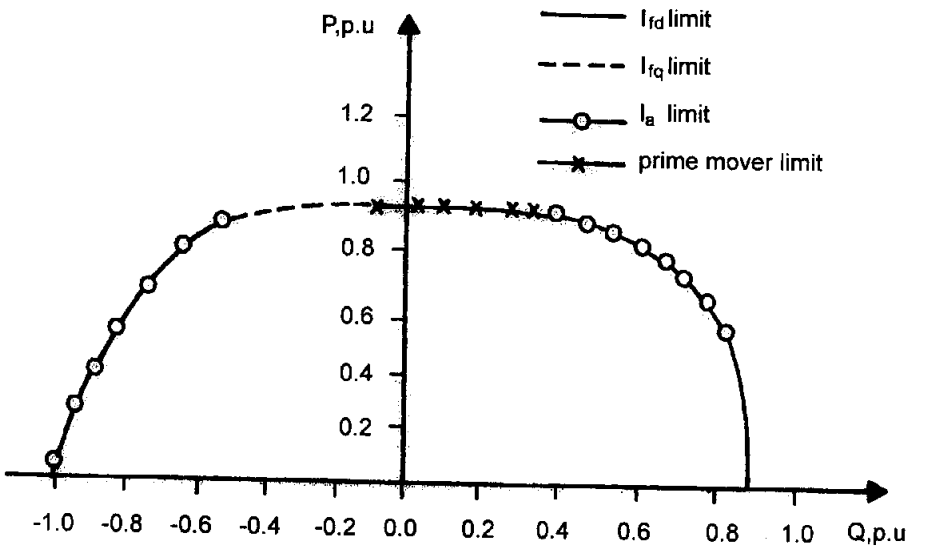

(a) Dual-excited

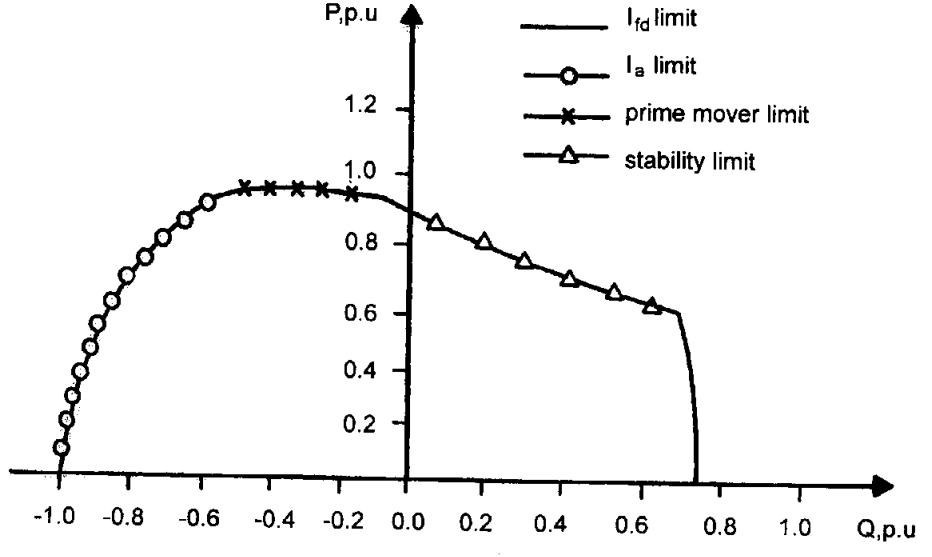

(b) Single excited

Fig. 18. Capability diagrams of the alternator.

Conclusions

Addition of an angle-regulated q-axis field winding to the synchronous generator improves the synchronizing torque, and also improves the self damping torque when the machine is not lightly loaded. The performance of the dual excited alternator is very sensitive to the gain of its AAR and the type of feedback. Positive feedback is acceptable over all the operating conditions region, while negative feedback leads to unstable operation at leading power factor loads. The magnetic saturation increases the synchronizing torque coefficient, but it decreases the damping torque coefficient. To avoid heating problems, machine designers should take care of the unexpected high values of the d-axis field current of the dual alternators resulting from the saturation effects.

References

[1] Adkins, B. and Harley, R.G. *The General Theory of Alternating Current Machines*. London: Chapman and Hall, 1975.

[2] Kapoor, S.C., Kalsi, S.S. and Adkins, B. "Improvement of Alternator Stability by Controlled Quadrature Excitation". *Proc. IEE*, 116, No.5 (May 1969), 771-780.

[3] Aggarwal, R.K. "Performance of Dual Excited Synchronous Generator at Leading Power Factors". *Proc. IEE*, 112, No.8 (Aug. 1975), 813-818.

[4] El-Serafi, A.M. and Badr, M.A. "Limitation of Increasing the Capacitate Power Loading of Regulated Dual Excited Synchronous Condensers". *IEEE PES Winter Meeting*, New York: N.Y. Jan. 28 - Feb. 2, 1973.

[5] El-Serafi, A.M. and Badr,M.A. "Extension of the Under Excited Stable Region of the Dual Excited Synchronous Machine". *IEEE Trans.*, PAS-92, No.1 (Jan. - Feb. 1973), 287-295.

[6] Doherety, R.E., and Nickle, C.A. "Synchronous Machine - Part III". *AIEE Trans. Power Apparatus and Systems*, 46 (Feb. 1927), 1-18.

[7] DeOliveria, S.E.M. "Effect of Excitation Systems and Power System Stabilisers on Synchronous Generator Damping And Synchronising Torques". *Proc. IEE*, 136, Pt. C, No. 5 (Sept. 1989), 264-270.

[8] Shaltout, A.A. and Abdel-Halim, M.A. "Damping and Synchronizing Torques of Salient-pole Generators with Accurate Representation of Stauration". *IEEE Trans. on Energy Conversion*, 10, Pt.1 (1995), 1-7.

[9] Garg, V., Demerdash, N. and Grisby, L. "Generalized Non-linear Synchronous Machine Model with Parametrs based on Design Particulars". *IEEE-PES Winter Meeting*, New York, Jan. 26-31, 1975.

[10] Subbarrao, N., Bursdge, E. and Finadlay, R. "Mathematical Models of Synchronous Machines for Dynamic Studies". *IEEE-PES Winter Meeting*, New York, Feb. 4-9, 1979.

[11] Soper, J.A., and Fagg, A.R. "Divided-winding Rotor Synchronous Generator". *Proc. IEE*, 116, No.1 (Jan. 1969), 113-126.

[12] Harley, R.G. and Adkins, B. "Stability of Synchronous Machine with Divided-winding Rotor". *Proc. IEE*, 117, No.5 (May 1970), 933-947.

[13] Abo-Shady, S.E., Ahmad, F.J., El-Hakim, S.M. and Badr, M.A. "Analysis of Self-dual Excited Synchronous Machine - Part I Development of the General Mathematical Model and Steady-state Performance Experimental Verification". *PES Summer Meeting*, San Francisco, July 12, 1987.

[14] Linville, T.M. "Starting Performance of Salient Pole Synchronous Motor". *AIEE Trans.*, (1930), 531-537.

[15] Rankin, A.W. "The Direct- and Quadrature-axis Equivalent Circuits of the Synchronous Machine". *AIEE Trans.*, (1945), 861-868.

[16] Manning, C.D. and Abdel-Halim, M.A. "A New Dynamic Inductance Concept and its Application to Synchronous Machine Modeling". *Proc. IEE*, 135, Pt. B, No.5 (Sept. 1988), 231-239.

[17] IEEE Committee Report "Excitation System Models for Power System Stability Studies". *IEEE Trans.*, PAS-100, No.2 (Feb. 1981), 494-509.

Appendix
Data of the System

Alternator parameters

494 KVA, 380 V, 4 bars/pole continuous ring damper winding, H = 3 sec. The equivalent circuit constants are as follows in p.u:

$X_{ad} = 1.418$	$X_{afd} = 1.311$	$X_{akld} = 0.740$
$X_{ak2d} = 1.110$	$X_{ffd} = 1.260$	$X_{kkld} = 0.612$
$X_{kk2d} = 0.953$	$r_a = 0.015$	$X_{ald} = 0.102$
$r_{fd} = 0.002$	$X_{fld} = 0.141$	$r_b = 0.047$
$X_b = 0.061$	$r_{rld} = 0.003$	$r_{r2d} = 0.005$
$X_{rld} = 0.0007$	$X_{r2d} = 0.001$	$r_{fq} = 0.002$
$X_{aq} = 0.630$	$X_{afq} = 0.560$	$X_{aklq} = 0.627$
$x_{ak2q} = 0.356$	$X_{ffq} = 0.550$	$x_{kk1q} = 0.676$
$k_{kk2q} = 0.334$	$X_{alq} = 0.105$	$r_{r1q} = 0.006$
$r_{r2q} = 0.004$	$X_{r1q} = 0.002$	$X_{r2q} = 0.001$

AVR Parametrs

$T_{RV} = 0.023$ sec., $T_{AV} = 0.22$ sec., $K_{AV} = 200$, $T_{FV} = 0.18$ sec, $K_{FV} = 0.016$, $E_{vx} = 19.9$ p.u
$E_{vn} = -19.9$ p.u

AAR Parameters

$T_{RA} = 0.023$ sec., $T_{AA} = 0.220$ sec., $K_{AA} = 0.5$, $T_{FA} = 0.18$ sec., $K_{FA} = 0.016$, $E_{Ax} = 19.9$ p.u
$E_{An} = -19.9$ p.u

Tie-Line Parameters

resistance = 0.05 p.u, reactance = 0.3 p.u

رسم المقدرة للمولد المتزامن ثنائي المجال معتبرًا التشبع المغناطيسي

عبدالحميد عبدالوهاب العوهلي و محمد عبدالسميع عبدالحليم

قسم الهندسة الكهربائية ، جامعة الملك سعود ، ص ب ٨٠٠،

الرياض ١١٤٢١، المملكة العربية السعودية

(استلم في ١٩٩٩/١١/٢٠م ، وقبل للنشر في ٢٠٠٠/٠٤/٢٦م)

ملخص البحث. طوّرت المولدات المتزامنة ذات المجال الثنائي لتحسين استقرارية أنظمة القوى الكهربائية. ويقدم هذا البحث دراسة دقيقه للاستقرار الديناميكي لهذه المولدات. ويعتمد تقدير الاستقرارية على حساب معاملي عزم التزامن وعزم الإخماد. ويمثل المولد بدائرة مكافئة مفصلة بها يحكي تمثيل التشبع بدقة وباستخدام هذه الدائرة أمكن حساب معاملات العزوم بتطبيق خوارزمي أقل المربعات على تغيرات الكميات الميكانيكية للمولد مع الزمن ، ومن ثم أمكن تحديد حدود الاستقرارية الديناميكية للمولد مع وجود منظم الجهد الأتوماتيكي وبتنظيم الزاوية الأتوماتيكية ، وبإضافة حدود التشغيل المفروضة على المولد نتيجة للقيود الحرارية والميكانيكية أمكن تعيين رسم المقدرة للمولد .